

# ACCEPTED VERSION

Anthony Miller and Yvonne Stokes

## **Simple analysis of line packing, attenuation, and rarefaction phenomena in water hammer**

Journal of Hydraulic Engineering, 2017; 143(10):06017017-1-06017017-8

© 2017 American Society of Civil Engineers.

This material may be downloaded for personal use only. Any other use requires prior permission of the American Society of Civil Engineers. This material may be found at: [http://dx.doi.org/10.1061/\(ASCE\)HY.1943-7900.0001367](http://dx.doi.org/10.1061/(ASCE)HY.1943-7900.0001367)

### **PERMISSIONS**

<http://ascelibrary.org/page/informationforasceauthorsreusingyourownmaterial>

### **Draft Manuscript**

Authors may post the final draft of their work on open, unrestricted Internet sites or deposit it in an institutional repository when the draft contains a link to the bibliographic record of the published version in the [ASCE Library](#) or [Civil Engineering Database](#). "Final draft" means the version submitted to ASCE after peer review and prior to copyediting or other ASCE production activities; it does not include the copyedited version, the page proof, or a PDF of the published version.

**15 March 2021**

<http://hdl.handle.net/2440/129891>

# Simple analysis of line packing, attenuation and rarefaction phenomena in water hammer

Anthony Miller <sup>1</sup> and Yvonne Stokes <sup>2</sup>

## ABSTRACT

The classical Joukowsky formula for the pressure jump associated with a sudden flow stoppage is a common engineering rule-of-thumb that is widely used to help estimate peak surge pressures, both positive and negative, in pipelines. However, strictly speaking, the Joukowsky result only holds at the moment of stoppage and at the point of stoppage. Whilst this is usually of little concern for short pipelines, the effects of pipe friction can cause significant deviations for long pipelines and for high frictional flows, where rarefaction and line packing phenomena can be critical. In this paper a number of extensions of the classical Joukowsky formula are described that take such frictional effects into account. By using suitable non-dimensional variables based on the system parameters, a single “universal” formulation of the underlying water-hammer equations is developed. The solution of these equations is presented both graphically and by way of some simple analytic approximations. Both instantaneous and finite duration stoppages of flow are considered. A finite shutdown can often usefully be thought as being intermediate between two instantaneous shutdown cases, one occurring at the start of the finite shutdown period, and the other at the finish. The intuitive notion that a finite shutdown period has a moderating effect on the subsequent development of rarefaction is shown to be incorrect for long pipelines.

**Keywords:** water hammer, Joukowsky formula, rarefaction, linepacking

---

<sup>1</sup>Flinders Mathematical Sciences Laboratory, Flinders University of South Australia, Tonsley SA 5042.  
Email: tony.miller@flinders.edu.au

<sup>2</sup>School of Mathematical Sciences, University of Adelaide, Adelaide SA 5005.  
Email: yvonne.stokes@adelaide.edu.au

## INTRODUCTION

The classical one-dimensional theory of water hammer was largely developed over a few decades spanning the late 19th and the early 20th centuries. Despite its simplicity, this theory continues to be successfully applied to analyse and design surge protection for large pipeline systems that transport a wide variety of important fluids such as water and oil (Chaudhry 2014). Within pipeline networks pressure surges can arise as a result of intentional events, such as flow start-up and shut down, or the opening or closing of a valve; or in response to unintentional events, such as a pump or valve failure. These events initiate pressure surges, both positive and negative, which travel through the network. These surges can cause considerable damage to pipeline infrastructure, and in some circumstances can be catastrophic. One of the great successes of the classical theory has been to predict the speed of propagation and the initial amplitude of the pressure surge resulting from the sudden halting of the flow at some point in a pipeline. This result usually goes by the name of Joukowsky's formula, and was first proposed by Nickolai Joukowsky in 1897 based on his experiments on the Moscow drinking water pipe network (Lüdecke and Kothe 2006).

Friction plays a significant role in the theory. The classical theory uses the semi-empirical Darcy-Weisbach friction factor. This factor is usually treated as a constant, meaning that the friction is modelled as proportional to the square of the flow velocity. (This is the principal source of nonlinearity in the classical water hammer theory.) Strictly speaking, however, the Darcy-Weisbach friction factor is only defined for steady state conditions, and moreover is not a constant, but depends on the flow velocity through the Reynolds number  $Re$ . Its use in the transient water hammer equations is therefore open to some question. Modern formulations sometimes employ more sophisticated friction models.

In the absence of friction, the initial Joukowsky pressure surge and associated velocity drop propagate unattenuated along the pipe, with the fluid being brought to rest once the surge has passed. With friction present, however, this velocity drop is attenuated as the surge travels along the pipe. As a result, behind the surge, the fluid in the pipe will still have some momentum in its original flow direction, and the magnitude of this residual momentum increases with

50 distance from the initial stoppage as the damping effects of friction accumulate. This has  
51 a somewhat surprising consequence. Downstream from the site of the initial stoppage, the  
52 fluid will continue to draw away from the slower moving fluid behind it once the surge has  
53 passed, leading to what has been called rarefaction of the flow (assuming that there is no  
54 separation of the flow column). This may eventually result in pressure falls which are several  
55 times that predicted by the Joukowsky result. Likewise on the upstream side, the fluid will not  
56 be completely stopped by the travelling surge and will continue to move towards the site of the  
57 initial stoppage, resulting in an increasing accumulation of fluid and a rise in pressure, that  
58 again may be several times that predicted by the Joukowsky result (Kaplan et al. 1967). This  
59 phenomenon has been called line-packing. At first glance, it seems a little unexpected that  
60 frictional damping leads to more extreme pressure transients than would be the case without  
61 friction.

62 These closely related concepts of line-packing, rarefaction and attenuation have been dis-  
63 cussed in the literature, particularly in relation to long pipelines and high frictional flows. Oil  
64 pipelines often fall into this category, (Chaudhry 2014), (Kaplan et al. 1967). However, most of  
65 this discussion has been rather qualitative, or has relied on numerical simulations of particular  
66 cases, typically based on the method of characteristics, to illustrate the concepts. There seems  
67 to have been little attention paid to addressing these topics analytically or from a more theo-  
68 retical point of view. Exceptions include (Leslie and Tijsseling 2000), which looks at frictional  
69 attenuation, and (Yao et al. 2015), which considers the long term attenuation of the successive  
70 reflections of the surges in short pipelines.

71 Numerical methods based on the method of characteristics solution of the water hammer  
72 equations are widely used to analyse pipeline transients. They are able to model complex  
73 pipeline networks with a variety of complex boundary conditions and to incorporate a variety  
74 of friction models in a straightforward manner. Nonetheless, an analytical or semi-analytical  
75 analysis of some simple pipeline configurations is still of value. Analytical expressions can  
76 reveal the physically significant parameters and parameter groupings and quantify how they  
77 influence the response of a system. In this way, they are more general than specific numerical

simulations, and thereby provide a more general understanding and insight.

This note describes some simple analytical approximations and semi-analytical solutions relevant to line packing, rarefaction and surge attenuation in long pipelines. They can be thought of as being frictional corrections to the classical Joukowsky head jump formulae. The discussion in this note is primarily in terms of the downstream rarefaction effects. However, the results can be readily transferred to upstream line packing.

## NOTATION

Consider a one-dimensional representation of a long pipeline, with  $x$  denoting the distance along the pipe. Let  $V(x, t)$  and  $H(x, t)$  be the velocity and the hydraulic head averaged over the cross section of the pipe at position  $x$  and time  $t$ . The pipe cross section is assumed to be circular. The hydraulic head  $H$  is defined by

$$H = z + \frac{p}{\rho g},$$

where  $z$  is the vertical elevation above some reference elevation,  $p$  is the fluid pressure relative to some reference pressure – typically atmospheric pressure,  $g$  is the acceleration due to gravity, and  $\rho$  is the density of the fluid.

Modern derivations of the classical water hammer equations can be found in standard engineering hydraulics texts such as (Chaudhry 2014) and (Streeter and Wylie 1983). It is convenient to write these equations in terms of the non-dimensional variables

$$h = \frac{g}{aV_0} H, \quad v = \frac{V}{V_0}, \quad \hat{x} = \frac{fV_0}{2aD} x, \quad \hat{t} = \frac{fV_0}{2D} t.$$

Here  $D$  is the diameter of the pipe, assumed to be constant;  $V_0 \geq 0$  is the uniform flow velocity of the initial steady state;  $f$  is the friction factor and  $a$  is the speed of propagation of a pressure disturbance in the pipe-fluid system, sometimes referred to as the celerity.

In order to gain an appreciation for the likely values that the non-dimensional variables  $\hat{x}$  and  $\hat{t}$  will take in practical applications, consider the case of a 100 km water pipeline, with

102  $D = 1 \text{ m}$ ,  $f = 0.02$ ,  $a = 10^3 \text{ ms}^{-1}$  and  $V_0 = 1 \text{ ms}^{-1}$ . In non-dimensional terms, the length of  
 103 this pipeline would be  $\hat{x} = 1$ . Clearly, increasing  $f$  or  $V_0$ , or decreasing  $D$  or  $a$  will increase the  
 104 non-dimensional length.

The waterhammer equations become in non-dimensional form

$$\frac{\partial h}{\partial x} + v|v| + \frac{\partial v}{\partial t} = 0 \quad (1)$$

$$\frac{\partial v}{\partial x} + \frac{\partial h}{\partial t} = 0, \quad (2)$$

105 where, for economy of notation,  $x$  and  $t$  have been reused to represent the nondimensional  $\hat{x}$   
 106 and  $\hat{t}$  respectively.

107 In non-dimensional terms, the initial steady state can be expressed as

$$108 \quad v = 1, \quad h = -x. \quad (3)$$

109 By differentiating (1) with respect to  $t$  and (2) with respect to  $x$  and eliminating the mixed  
 110 derivative of  $h$ , the non-linear wave equation

$$111 \quad \frac{\partial^2 v}{\partial t^2} + \frac{\partial(v|v|)}{\partial t} = \frac{\partial^2 v}{\partial x^2} \quad (4)$$

112 is obtained.

113 Define the characteristic variables

$$114 \quad \xi = x - t, \quad \eta = x + t.$$

Transforming the derivatives in the original equations to derivatives with respect to  $\xi$  and  $\eta$ ,

and rearranging these equations gives

$$\frac{\partial h}{\partial \xi} - \frac{\partial v}{\partial \xi} + \frac{1}{2}v|v| = 0, \quad (5)$$

$$\frac{\partial h}{\partial \eta} + \frac{\partial v}{\partial \eta} + \frac{1}{2}v|v| = 0. \quad (6)$$

Figure 1 shows the orientation of the lines of constant  $\xi$  and constant  $\eta$  in the  $x$ - $t$  plane. Now integrating the first of the above equations along a line of constant  $\eta$  and the second along a line of constant  $\xi$  leads to

$$(h - v)\Big|_{\xi_0}^{\xi_1} = - \int_{\xi_0}^{\xi_1} \frac{1}{2}v|v| d\xi \quad (\eta = \text{constant}) \quad (7)$$

$$(h + v)\Big|_{\eta_0}^{\eta_1} = - \int_{\eta_0}^{\eta_1} \frac{1}{2}v|v| d\eta \quad (\xi = \text{constant}). \quad (8)$$

It is sometimes convenient to return to the original variables  $x$  and  $t$ ,

$$(h - v)\Big|_{x_0, t_0}^{x_1, t_1} = - \int_{x_0, t_0}^{x_1, t_1} v|v| dx \quad (x + t = \text{constant}) \quad (9)$$

$$(h + v)\Big|_{x_0, t_0}^{x_1, t_1} = - \int_{x_0, t_0}^{x_1, t_1} v|v| dx \quad (x - t = \text{constant}). \quad (10)$$

These equations are the basis of the method of characteristics for solving the water hammer equations.

A non-linear wave equation for  $v$  can be obtained in terms of the characteristic variables by differentiating (5) with respect to  $\eta$  and (6) with respect to  $\xi$ , and then eliminating the common mixed derivative of  $h$ . This gives

$$\frac{\partial^2 v}{\partial \xi \partial \eta} = \frac{1}{4} \left( \frac{\partial}{\partial \eta} - \frac{\partial}{\partial \xi} \right) (v|v|). \quad (11)$$

## INSTANTANEOUS STOPPAGE OF FLOW

## Some Analytical Solutions

Consider an infinite pipeline that has steady uniform flow as given by (3). Assume that at time  $t = 0$  the flow instantaneously stops at  $x = 0$ . For example, this stoppage could be due to the sudden closure of a valve, or a pump failure. This isolates the upstream and downstream flows, which now evolve independently.

The stoppage of flow at  $x = 0$  results in discontinuities in  $h$  and  $v$  which travel downstream at a non-dimensional speed of 1. As shown in Figure 2, this can be represented in  $x, t$  space as the characteristic line  $x = t$ , or  $\xi = 0$  in the notation that was introduced earlier. This line divides  $x, t$  space into two regions, representing points behind the surge ( $x < t$ ) and points in front of the surge ( $x > t$ ). In front of the surge, the steady uniform flow solution  $v = 1$ ,  $h = -x$  continues to satisfy (1) and (2). Let  $P$  be any point on the line  $x = t$ , and consider how  $h$  and  $v$  are related on either side of this line in  $x, t$  space near  $P$ . Let  $P'$  and  $P''$  be nearby points as in Figure 2 which lie on a line  $\eta = \text{constant}$ . Let  $P' \rightarrow P$  from in front of the surge, and  $P'' \rightarrow P$  from behind the surge, and apply (7) to obtain

$$\lim_{P'' \rightarrow P} (h - v) = \lim_{P' \rightarrow P} (h - v), \quad (12)$$

since the friction integral has a limiting value of 0 as the distance  $P'P'' \rightarrow 0$ . Note that the left hand limit is from behind the surge, and the right hand one is from in front of the surge. This result states that the discontinuous jumps in  $h$  and  $v$  across the surge are equal, which can be thought of as an extended Joukowski relation.

In front of the surge, the initial steady state distributions of  $h$  and  $v$  apply. These correspond to

$$v = 1, \quad h = -x. \quad (13)$$

Thus (12) gives

$$h - v = -x - 1, \quad (14)$$

where here  $h$  and  $v$  denote the limiting values at a point  $P$  on the characteristic  $x = t$  as it is



approached from behind the surge.

Next apply (6) along the characteristic  $x = t$ , using the limiting values for  $h$  and  $v$  from behind the surge. Use (14) to substitute directly for  $h$  to obtain

$$\frac{\partial}{\partial \eta}(-x - 1) + 2\frac{\partial v}{\partial \eta} + \frac{1}{2}v|v| = 0.$$

Noting that  $\eta = 2x$  on  $x = t$ , and supposing tentatively that  $v \geq 0$ , leads to the ordinary differential equation

$$\frac{dv}{d\eta} = \frac{1}{4}(1 - v^2),$$

the solution of which, corresponding to the initial condition  $v = 0$  at  $\eta = 0+$ , is

$$v = \tanh\left(\frac{\eta}{4}\right) = \tanh\left(\frac{x}{2}\right). \quad (15)$$

Using (14), the corresponding result for the head  $h$  is

$$h = -1 - x + \tanh\left(\frac{x}{2}\right). \quad (16)$$

Therefore the instantaneous changes in head and velocity that occur as the surge passes are

$$\Delta h = \Delta v = -1 + \tanh\left(\frac{x}{2}\right),$$

demonstrating the attenuation with distance due to friction. As  $x \rightarrow 0+$ , both  $\Delta h, \Delta v \rightarrow -1$ , which is just the classical Joukowsky result. At the other extreme, as  $x \rightarrow \infty$ , corresponding to a very long pipeline, both  $\Delta h, \Delta v \rightarrow 0$ , and so the effect of the initial stoppage at  $x = 0$  will be negligible at large distances. In such cases, any reflection at a downstream boundary may be negligible, (Kaplan et al. 1967). The results (15) and (16) are similar to some derived in (Leslie and Tijsseling 2000).

To progress further, suppose that  $x$  and  $t$  are small, and seek a Taylor series expansion for

167  $v$  in the region behind the surge,  $0 \leq x \leq t$ ,  $t \geq 0$ ,

$$168 \quad v(x, t) = \sum_{n=0}^{\infty} \sum_{k=0}^n a_{nk} x^k t^{n-k}.$$

Substitute this expansion into (4) and equate corresponding powers of  $x$  and  $t$ . Note also the conditions that pertain on the boundaries  $x = 0$  and  $x = t$  in Figure 2,

$$\begin{aligned} v(0, t) &= 0 \text{ for } t \geq 0 \\ v(x, x) &= \tanh\left(\frac{x}{2}\right) = \frac{x}{2} - \frac{x^3}{24} + \cdots, \end{aligned} \quad (17)$$

169 where in the last boundary condition  $v(x, x)$  is understood as the limiting value from behind the  
170 surge. It can be shown that these conditions are sufficient to uniquely determine the coefficients  
171  $a_{nk}$ . The first few terms of the expansion are

$$172 \quad v(x, t) = \frac{x}{2} + \left(-\frac{x^3}{96} - \frac{xt^2}{32}\right) + \cdots. \quad (18)$$

173 Although higher order terms can be calculated, there seems little practical value in doing so  
174 as their inclusion does not improve the convergence appreciably. In fact, it is not unexpected  
175 that this power series for  $v$  has restricted convergence. Firstly, the Taylor series (17) for the  
176 boundary condition only has a finite radius of convergence of  $\pi$ , as  $\tanh(x/2)$  has a singularity  
177 in the complex plane at  $x = \pm i\pi$ , corresponding to  $\tan(\pm\pi/2)$ . Also, by equating corresponding  
178 powers of  $x$  and  $t$  in (4), the implicit assumption is being made that  $x$ ,  $t$  and  $v^2$  are small.

179 To obtain a corresponding analytical expression for  $h$ , note that by (1) and (2)

$$180 \quad h(x, t) = h(0, 0) + \int_0^t -\frac{\partial v}{\partial x}(0, s) ds + \int_0^x -\left(v^2(s, t) + \frac{\partial v}{\partial t}(s, t)\right) ds. \quad (19)$$

181 By the Joukowsky formula,  $h(0, 0) = -1$ , and so after using (18) in the line integrals above and

grouping terms by powers of  $x$  and  $t$  it follows that

$$h(x, t) = -1 - \frac{t}{2} + \left( -\frac{x^3}{12} + \frac{x^2 t}{32} + \frac{t^3}{96} \right) + \dots \quad (20)$$

Retaining only the constant terms in (18) and (20) gives  $v(x, t) = 0$ ,  $h(x, t) = -1$ , which corresponds to the classical Joukowski result expressed in non-dimensional form. Thus, the formulae (18) and (20) can be thought of as higher order extensions of the classical Joukowski result.

### Comparison with Method of Characteristics Solution

In order to assess the accuracy of these approximations A straightforward numerical implementation of the method of characteristics based on (9) and (10) was used to solve (1) and (2), as described in (Streeter and Wylie 1983), for example. The discretisation steps used were  $\Delta t = \Delta x = \Delta = 0.01$ .

Figure 3 gives a detailed graphical representation of this solution for the downstream flow. This plot contains a lot of information, and so requires some explanation. The figure primarily shows head  $h$  and velocity  $v$  as functions of  $x$  for  $0 < x < 10$  at the non-dimensional times  $t = 0.5$ , and  $t = 1, 2, \dots, 9, 10$ . The scale for head is the left hand vertical axis, and velocity scale is the right hand vertical axis. The dashed black line is the head corresponding to the initial uniform steady flow (the hydraulic grade line). It is simply  $h = -x$ . Consider the head data that is shown as solid red curves. For each of the displayed  $t$  values, the head is given for  $0 < x < t$ . At  $x = t$ , the head will jump vertically to the hydraulic grade line. This discontinuity is associated with the passage of the initial surge. To avoid clutter on the plot, this vertical jump has not been explicitly shown. The dashed red line is the locus of head just after the initial surge has passed the point  $x = t$ . This is given by the analytic expression

$$h = -1 - x + \tanh(x/2), \quad (21)$$

as discussed in (16). Turn now to the velocity data, which is shown in blue in Figure 3. For

each of the displayed  $t$  values, the velocity is shown for  $0 < x < t$ . At  $x = t$ , the velocity will jump vertically to  $v = 1$ . Again for clarity, this discontinuity has not be shown. The dashed violet line shows the locus of velocity immediately after the initial surge has passed the point  $x = t$ . Again there is an analytic expression for this,

$$v = \tanh(x/2), \quad (22)$$

as discussed in (15). Note that in the figure the velocity curves for  $t = 0.5, 1$  are partially obscured as they are almost coincident with the dashed violet line.

Figure 4 shows an exploded view for  $0 < x < 2.5$ , which is likely to be the most common part of the range covered by Figure 3, at least for water pipelines. Comparing the analytical approximations (18) and (20) with this method of characteristics solution shows that the analytical approximations are visually identical to the solutions in Figure 4 for  $0 \leq x \leq t < 1$ , while they are probably acceptably close for most practical purposes for the range  $0 \leq x \leq t < 2$ .

Incidentally, Figures 3 and 4 are some interest in their own right as they provide a compact graphical summary of the magnitude of the attenuation and rarefaction phenomena and how they depend on system parameters.

## THE CASE OF A FINITE SHUTDOWN TIME

Until now the stoppage of the flow at  $x = 0$  has been assumed instantaneous. Realistically, however, the fluid at  $x = 0$  will come to rest over some finite period of time. Intuitively, it might be expected that a finite shutdown time should reduce the transient peaks in head that are associated with a sudden shutdown. On the other hand, for the frictionless case, a finite shutdown time leads to the same Joukowsky drop in head as an instantaneous stoppage, but with a time delay. This section will seek to better understand and quantify the effect of a finite shutdown period on the subsequent flow for the idealised case of an infinitely long pipe. Note that the duration of the shutdown period, and also the velocity versus time profile at  $x = 0$  during this shutdown, are unlikely to be known with much certainty, particularly if the cause

of the shutdown is an unexpected failure event. Thus, wherever possible, minimal assumptions will be made concerning the shutdown profile.

Consider the case of a flow disruption at  $x = 0$  that brings the flow to rest at  $x = 0$  during the (non-dimensional) time period  $0 \leq t \leq \tau$  according to  $v(0, t) = \phi(t/\tau)$ ,  $0 \leq t \leq \tau$ . It will be assumed that the velocity profile function  $\phi$  is a non-increasing function of its argument between 0 and 1, with  $\phi(0) = 1$  and  $\phi(1) = 0$ . This case is depicted in the  $x, t$  space plot in Figure 5. The approach that will be taken is to first solve the water hammer equations in the surge zone  $D_0$  of the figure, using the known boundary conditions on the leading edge characteristic  $x = t$  and on the  $t$ -axis segment  $x = 0$ ,  $0 \leq t \leq \tau$  (marked by bold in the figure). This solution will supply a boundary condition on the trailing edge characteristic  $x = t - \tau$ ,  $t \geq \tau$ , which can then be used to solve the water hammer equations on the angular region  $D_1$ , much as in the previous section.

### Some Analytical Solutions

Consider the wave equation (11) in the characteristic variables  $\xi$  and  $\eta$  in the surge region  $D_0$  and provisionally assume that  $v \geq 0$ . Seek a solution using the iteration

$$\frac{\partial^2 v_{n+1}}{\partial \xi \partial \eta} = \frac{1}{4} \left( \frac{\partial}{\partial \eta} - \frac{\partial}{\partial \xi} \right) v_n^2, \quad n = 0, 1, \dots,$$

starting with  $v_0(\xi, \eta) = \phi(-\xi/\tau)$ , where  $\phi$  is the shutdown velocity profile defined previously. Note that  $v_0$  satisfies the boundary conditions of the original problem on the boundary segments of  $D_0$  marked in bold in Figure 5, and also  $\partial^2 v_0 / \partial \xi \partial \eta = 0$  on  $D_0$ . (In fact,  $v_0$  is the frictionless solution.) It is convenient to write

$$w_0 = v_0, \quad w_1 = v_1 - v_0, \quad w_2 = v_2 - v_1, \dots,$$

so that  $v_n = w_0 + w_1 + \dots + w_n$ . The above iteration can then be written

$$\begin{aligned}\frac{\partial^2 w_1}{\partial \xi \partial \eta} &= \frac{1}{4} \left( \frac{\partial}{\partial \eta} - \frac{\partial}{\partial \xi} \right) w_0^2, \\ \frac{\partial^2 w_n}{\partial \xi \partial \eta} &= \frac{1}{4} \left( \frac{\partial}{\partial \eta} - \frac{\partial}{\partial \xi} \right) \left( 2w_{n-1} \sum_{k=0}^{n-2} w_k + w_{n-1}^2 \right), \quad n = 2, 3, \dots\end{aligned}$$

This may be solved sequentially for  $w_k$ ,  $k = 1, 2, \dots$  on  $D_0$  with each  $w_k = 0$  on the boundary segments marked in bold in the figure.

The first two instances of the above iteration are

$$\begin{aligned}\frac{\partial^2 w_1}{\partial \xi \partial \eta} &= \frac{1}{4} \left( \frac{\partial}{\partial \eta} - \frac{\partial}{\partial \xi} \right) w_0^2, \\ \frac{\partial^2 w_2}{\partial \xi \partial \eta} &= \frac{1}{4} \left( \frac{\partial}{\partial \eta} - \frac{\partial}{\partial \xi} \right) (2w_0 w_1 + w_1^2).\end{aligned}$$

Solve these for  $w_1$  and  $w_2$  in turn, each time integrating successively with respect to  $\eta$  and  $\xi$  and then applying the zero boundary conditions. This gives

$$\begin{aligned}w_0(\xi, \eta) &= \phi \left( -\frac{\xi}{\tau} \right) \\ w_1(\xi, \eta) &= \left( 1 - \phi^2 \left( -\frac{\xi}{\tau} \right) \right) \frac{(\xi + \eta)}{4} \\ w_2(\xi, \eta) &= -\frac{(\xi + \eta)\tau}{16} \int_0^{-\xi/\tau} a(s) ds + \frac{(\xi + \eta)\tau^2}{32} \int_0^{-\xi/\tau} s b(s) ds - \frac{(\eta^2 - \xi^2)\tau}{64} \int_0^{-\xi/\tau} b(s) ds \\ &\quad - \frac{(\xi + \eta)^2}{32} a \left( -\frac{\xi}{\tau} \right) - \frac{(\xi + \eta)^3}{192} b \left( -\frac{\xi}{\tau} \right)\end{aligned}$$

where  $a(s)$ ,  $b(s)$ , which are defined for  $0 \leq s \leq 1$  by

$$a(s) = 2\phi(s)(1 - \phi^2(s)), \quad b(s) = (1 - \phi^2(s))^2,$$

depend only on the shutdown profile  $\phi$ .

Noting that  $\xi + \eta = 2x$  and  $\eta^2 - \xi^2 = 4xt$ , it follows that on the the trailing edge  $\xi = -\tau$  of

the surge zone  $D_0$ , where  $t = x + \tau$ ,

$$v(x, x + \tau) = \frac{x}{2} - \left( \frac{A\tau}{8} + \frac{(B - M)\tau^2}{16} \right) x - \frac{B\tau}{16} x^2 - \frac{x^3}{24} + \dots, \quad (23)$$

where  $A$ ,  $B$  and  $M$  are constants, depending only on the shutdown profile function  $\phi$ , and defined by

$$\begin{aligned} A &= \int_0^1 a(s) ds = \int_0^1 2\phi(1 - \phi^2) ds \\ B &= \int_0^1 b(s) ds = \int_0^1 (1 - \phi^2)^2 ds \\ M &= \int_0^1 sb(s) ds = \int_0^1 s(1 - \phi^2)^2 ds \end{aligned}$$

To find  $h(0, \tau)$ , use (2) to obtain

$$\begin{aligned} h(0, \tau) &= - \int_0^\tau \frac{\partial v}{\partial x}(0, s) ds \\ &= -1 - \frac{G^*\tau}{2} + \frac{A^*\tau^2}{8} + \frac{Q^*\tau^3}{16} + \dots, \end{aligned} \quad (24)$$

where

$$\begin{aligned} G^* &= \int_0^1 (1 - \phi^2) ds, \\ A^* &= \int_0^1 \int_0^t a(s) ds dt = \int_0^1 \int_0^t 2\phi(1 - \phi^2) ds dt \\ Q^* &= \int_0^1 \int_0^t (t - s)b(s) ds dt = \int_0^1 \int_0^t (t - s)(1 - \phi^2)^2 ds dt \end{aligned}$$

are again constants that depend only on the shutdown profile function  $\phi$ .

As might be expected, in the limit as  $\tau \rightarrow 0$ , the expression (23) agrees with the first two terms of the Taylor expansion of  $\tanh(x/2)$  which appears in the boundary condition (17) for the instantaneous stoppage case. In addition, (24) becomes  $h(0, 0) = -1$ , which is just the classical Joukowsky result. For the particular case of a linear profile the coefficients  $A = 0.5$

and  $G^* = 2/3$ . Retaining only the terms that are first order in  $\tau$ ,

$$v(x, x + \tau) \approx \frac{x}{2} \left(1 - \frac{\tau}{8}\right) - \frac{x^3}{24}, \text{ and } h(0, \tau) \approx -1 - \frac{\tau}{3}.$$

The results (23) and (24) provide the  $v$  and  $h$  boundary conditions needed to solve the water hammer equations (1) and (2) in the angular region  $D_1$ . Proceeding as in the previous section, assume a power series expansion for  $v$ , substitute this into (4) and equate corresponding powers of  $x$  and  $t$ . It is natural to use the shifted non-dimensional time  $t^* = t - \tau$  in place of  $t$ . It follows that for the region  $0 \leq x \leq t^*$ ,  $t^* \geq 0$

$$v(x, t) = \Lambda(\tau) \frac{x}{2} - \frac{B\tau}{16} x t^* - \frac{x^3}{96} - \frac{x t^{*2}}{32} + \dots \quad (25)$$

$$h(x, t) = -1 - \mathcal{J}(\tau) - \Lambda(\tau) \frac{t^*}{2} + \frac{B\tau}{32} (x^2 + t^{*2}) - \frac{\Lambda^2(\tau)}{12} x^3 + \frac{x^2 t^*}{32} + \frac{t^{*3}}{96} + \dots, \quad (26)$$

where

$$\mathcal{J}(\tau) = \frac{G^* \tau}{2} - \frac{A^* \tau^2}{8} - \frac{Q^* \tau^3}{16}, \text{ and } \Lambda(\tau) = 1 - \frac{A\tau}{4} - \frac{(B - M)\tau^2}{8}.$$

Observe that in the limit of an instantaneous stoppage as  $\tau \rightarrow 0$ , these results agree with those derived previously. Another way to think about an instantaneous stoppage at  $t = 0$  is as a shutdown of finite duration  $\tau$  with a profile  $\phi$  that is a step function at  $t = 0$  with  $\phi(0) = 1$  and  $\phi(s) = 0$  for  $0 < s \leq 1$ . The various integrals defined above then become  $A = 0, B = 1, M = 0.5, G^* = 1, A^* = 0$  and  $Q^* = 1/6$ . Substituting into (25) and (26) leads again to agreement with (18) and (20), at least up to cubic terms in  $x, t$ . More generally, it can be shown that a unit step change in velocity occurring at anytime between  $t = 0$  and  $t = \tau$  will give similar agreement between the results (25, 26), and (18, 20). This is further evidence of the consistency between the results of this and the previous section. Because of this agreement, the convergence of (25) and (26) will also be restricted, both for  $x, t$ , and for  $\tau$ .

Considering only the terms of (25) and (26) that are first order in  $t, \tau$  or  $x$ , gives

$$v = \frac{x}{2} + \dots \text{ and } h = -1 - \frac{G^* \tau}{2} - \frac{t^*}{2} + \dots. \quad (27)$$



From the definition of  $G^*$  it can be seen that for any shutdown velocity profile  $\phi$ , the integral  $0 \leq G^* \leq 1$ , and so at the shifted time  $t^* = 0$  ( $t = \tau$ ), the approximation (27) gives a head drop  $-1 - \tau/2 \leq h \leq -1$ . The first order head drop at  $t = \tau$  for an instantaneous stoppage at  $t = 0$  is given by (20) as  $h = -1 - \tau/2$ . Thus, a finite shutdown results in a slightly smaller “initial” head drop at  $\tau = 0$  than a instantaneous stoppage; however, both (27) and the first order terms of (20) then show an ongoing fall in  $h$  with time at a non-dimensional rate of  $1/2$ . Thus, to this first order level of approximation, a finite shutdown period has no significant moderating effect on the development of rarefaction within a long pipeline. The intuitive notion that a finite shutdown time should significantly moderate the rarefaction depends upon the effect of reflections, which will only be present for finite length pipelines (that is, pipelines of non-dimensional length comparable to  $\tau$ ).

### Comparison with Method of Characteristics Solution

Figure 6 shows the results of a numerical method of characteristics solution for the case  $\tau = 0.25$ . This shows  $h(x, t)$  and  $v(x, t)$  for  $t = 0.5, 1$  and  $2$  as the solid lines. For  $t = 0.5$  and  $1$  the curves are visually indistinguishable from the approximations given by (25) and (26); indeed, the simpler approximations (27) would be adequate for practical purposes. The  $t = 2$  curves are closely approximated by (25) and (26).

Figure 6 also shows  $h(x, t)$  and  $v(x, t)$  for some corresponding cases of instantaneous shutdowns are shown as dashed lines. The two dashed curves bracketing the solid lines represent instantaneous shutdowns at  $t = 0$  (lower dashed curve) and  $t = \tau$  (upper dashed curve) respectively. It is seen that each of the head curves for the finite shutdown case is bracketed between the head curves for the two instantaneous shutdown cases. This seems physically reasonable, as the finite shutdown is intermediate between an instantaneous stoppage at time  $t = 0$  and a delayed instantaneous stoppage occurring at time  $t = \tau$ , with the latter producing a weaker rarefaction, simply because the flow has been halted later in time and so has not had as much time to develop cumulative rarefaction. This again supports the observation made earlier that, in the absence of reflections arising from a finite length pipeline, a finite shutdown time has no significant moderating influence on the head transients.

## CONCLUSION

Engineering rules-of-thumb are often helpful at the preliminary stage of surge protection design, and also at the later, more detailed stages, when they assist with the understanding and interpretation of the results of computer simulations and other detailed calculations. They are also useful for assessing parameter sensitivity. The classical Joukowsky formula for the pressure jump associated with a sudden flow shutdown is one such rule-of-thumb that is widely used to estimate expected surge pressure peaks, both positive and negative, in pipelines. However, strictly speaking, the Joukowsky result only holds at the moment of stoppage and at the point of stoppage. Whilst this is usually of little concern for short pipelines, the effects of pipe friction can cause significant deviations for long pipelines and for high frictional flows. In this paper a number of extensions of the classical Joukowsky formula have been described that take such frictional effects into account. These extensions are relatively easy to apply, and require little extra calculation. They can still be considered practical rules-of-thumb.

By using suitable non-dimensional variables based on the system parameters, a single “universal” formulation of the underlying water-hammer equations is developed that is applicable to long pipelines. The complete solution of these equations has been presented in a single chart, which can be used to estimate head and velocity at any point and time during the initial surge following a stoppage event. Aside from this graphical representation, analytic expressions are also derived, which are valid for medium length pipes. For the case of a long pipeline, a simple approximation to the head behind the surge is given in non-dimensional terms by  $h = -1 - t/2$ , which is independent of  $x$ . Note that the corresponding non-dimensional formulation of the classical Joukowsky relation is  $h = -1$ .

In practice, flow stoppage occurs over a finite shutdown period. This is also addressed in this paper and analytic expressions are also derived for this case. Often the precise details of a pipeline shutdown event, such as its duration and the velocity-time profile are only known in approximate terms, particularly if the event is unplanned or accidental. This makes any detailed specific analysis somewhat artificial, as there is little firm data upon which to base such an analysis. In examples presented here, it is suggested that often the features of the surge

that are important are relatively insensitive to the fine details of the shutdown. A sufficiently accurate analysis may often be based on considering a finite shutdown as being intermediate between two instantaneous shutdown cases, one occurring at the start of the finite shutdown period, and the other at the end. The intuitive notion that a finite shutdown period has a moderating effect on the subsequent development of rarefaction is shown to be incorrect for long pipelines.

The analysis considered here is restricted to looking at the initial, outward travelling surge, before any reflection events occur at reservoirs or other pipeline components. Although this is an obvious restriction, this initial pressure surge is often the most critical, particularly for long pipelines, and so the simple analysis presented here, which extends the classical Joukowski result, should be useful.

## REFERENCES

- Chaudhry, M. H. (2014). *Applied Hydraulic Transients*. Springer, 3rd edition.
- Kaplan, M., Streeter, V. L., and Wylie, E. B. (1967). "Computation of oil pipeline transients." *Journal of the Pipeline Division, Proceedings of the American Society of Civil Engineers*, 93(PL3), 59–72.
- Leslie, D. J. and Tijsseling, A. S. (2000). "Travelling discontinuities in waterhammer theory – attenuation due to friction." *BHR Group, Proc. of the 8th International Conference on Pressure Surges*, A. Anderson, ed., London, UK, Professional Engineering Publishing, 323–335 (April). Available at [http://www.win.tue.nl/~tijssel/pdf\\_files/Leslie-Tijsseling\\_2000.pdf](http://www.win.tue.nl/~tijssel/pdf_files/Leslie-Tijsseling_2000.pdf).
- Lüdecke, H.-J. and Kothe, B. (2006). "Water hammer. KSB Know-how, Volume 1, published by KSB Aktiengesellschaft Communications, Halle (Germany). Available at [http://www.ksb.com/ksb-en/Products\\_and\\_Services/building-services/Planer-Tools/Know-how\\_Broschueren/](http://www.ksb.com/ksb-en/Products_and_Services/building-services/Planer-Tools/Know-how_Broschueren/).
- Streeter, V. L. and Wylie, E. B. (1983). *Fluid Mechanics*. Civil and Mechanical Engineering Series. McGraw Hill, first SI metric edition.
- Yao, E., Kember, G., and Hansen, D. (2015). "Analysis of water hammer attenuation in appli-

389 cations with varying valve closure times.” *J. Eng. Mech.*, 141 DOI:10.1061/(ASCE)EM.1943-  
390 7889.0000825.

## List of Figures

- 1 The orientation of the characteristic variables  $\xi = x - t$ ,  $\eta = x + t$ . . . . . 21
- 2 Derivation of an extended Joukowski relation for the discontinuities in head and velocity across a travelling surge. . . . . 22
- 3 Graphical representation of the downstream solutions for  $h$  (solid red) and  $v$  (solid blue) following the instantaneous stoppage of flow at  $x = 0$ ,  $t = 0$ . Results are shown for  $0 < x \leq t$  for the non-dimensional times  $t = 0.5$  and  $t = 1, \dots, 10$  (in steps of 1). The black dashed line is the initial hydraulic grade line, and the dashed red and purple lines are the values of  $h$  and  $v$  respectively, immediately after the initial (negative) surge has passed  $x = t$ . (The purple dashed line partially obscures the  $v = 0, 5, 1$  curves.) See the text for further details. . . . . 23
- 4 An expanded view of Figure 3 in the region  $0 < x < 2.5$ . This is the non-dimensional region which will apply for many water pipelines. . . . . 24
- 5 Derivation of an extended Joukowsky relation for the changes in head and velocity across a travelling surge for the case of a finite shutdown time. Here  $\phi(t/\tau)$  is the velocity profile at  $x = 0$  during the shutdown period  $0 \leq t \leq \tau$ .  $D_0$  is the subsequent surge zone in  $x, t$  space. . . . . 25
- 6 Plots of the downstream  $h$  (red) and  $v$  (blue) for a finite shutdown time of  $\tau = 0.25$ . (A linear shutdown velocity profile  $\phi$  has been assumed.) The red and blue dashed lines bracketing the solid lines correspond to instantaneous shutdowns occurring at  $t = 0$  (below) and  $t = \tau$  (above). To prevent clutter in the figure, the discontinuous jumps in  $h$  and  $v$  for the instantaneous shutdowns have not been shown; also, the bracketing curves for velocity are only shown for  $t = 2$ . The dashed black line is the hydraulic grade line,  $h = -x$ . . . . . 26

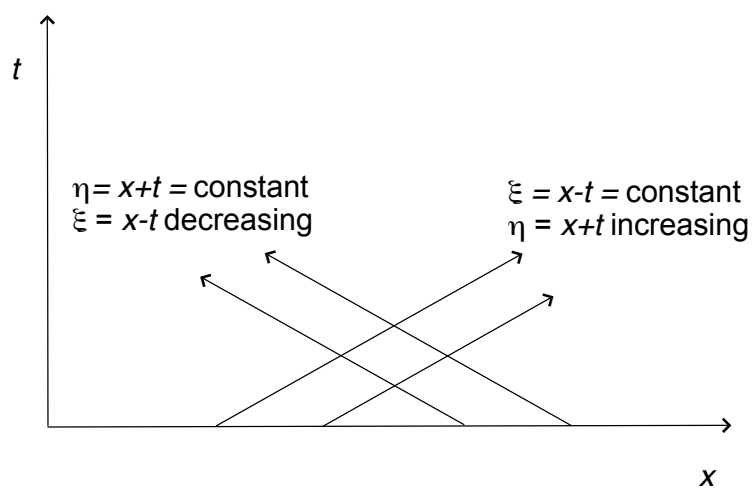


**FIG. 1.** The orientation of the characteristic variables  $\xi = x - t$ ,  $\eta = x + t$ .

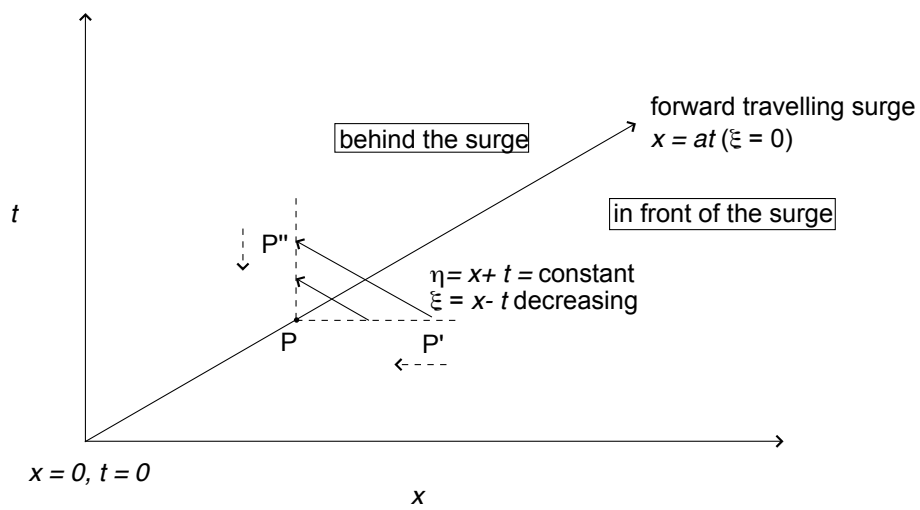


**FIG. 2.** Derivation of an extended Joukowski relation for the discontinuities in head and velocity across a travelling surge.

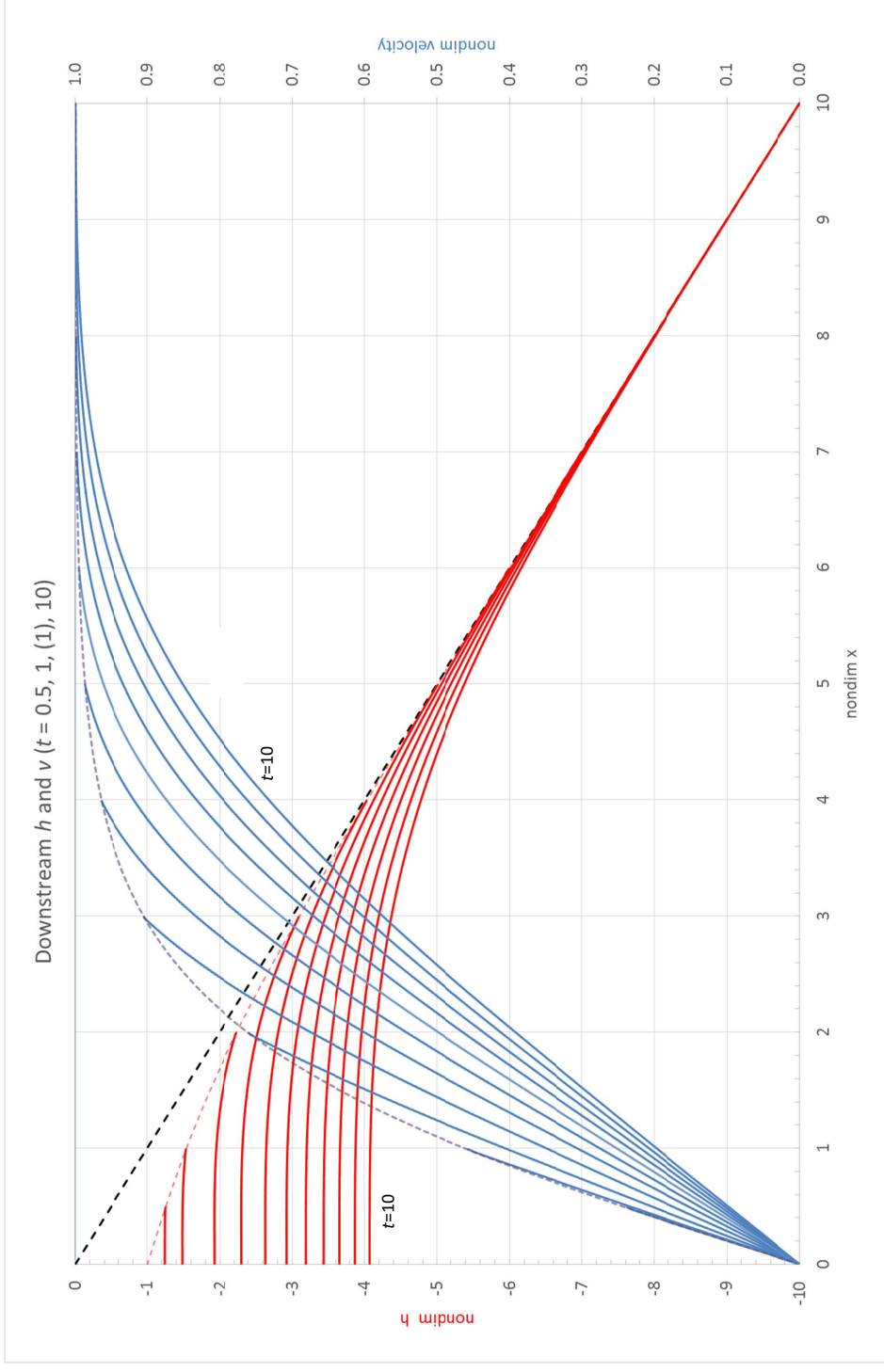


**FIG. 3.** Graphical representation of the downstream solutions for  $h$  (solid red) and  $v$  (solid blue) following the instantaneous stoppage of flow at  $x = 0$ ,  $t = 0$ . Results are shown for  $0 < x \leq t$  for the non-dimensional times  $t = 0.5$  and  $t = 1, \dots, 10$  (in steps of 1). The black dashed line is the initial hydraulic grade line, and the dashed red and purple lines are the values of  $h$  and  $v$  respectively, immediately after the initial (negative) surge has passed  $x = t$ . (The purple dashed line partially obscures the  $v = 0, 5, 1$  curves.) See the text for further details.



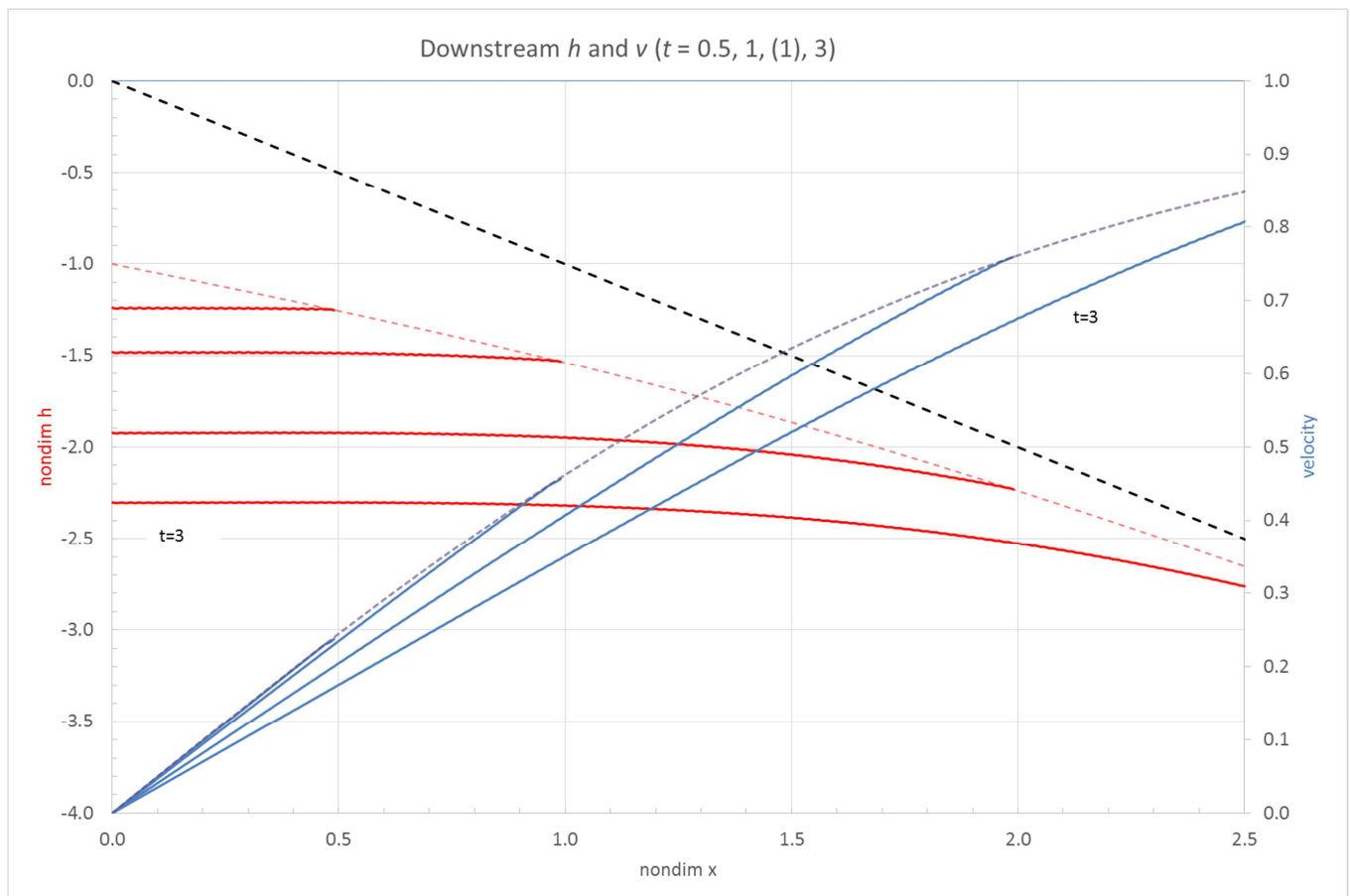


**FIG. 4.** An expanded view of Figure 3 in the region  $0 < x < 2.5$ . This is the non-dimensional region which will apply for many water pipelines.

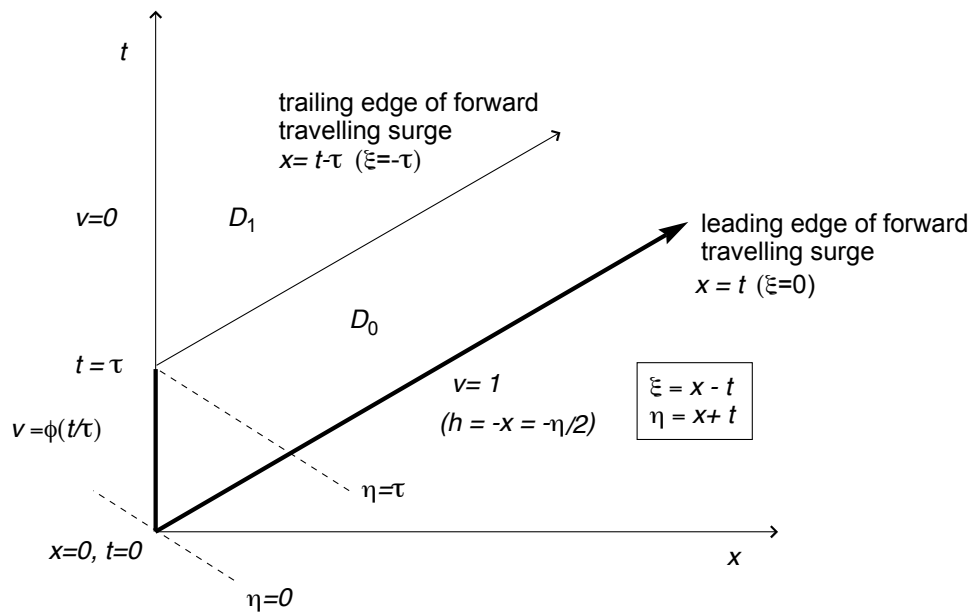


**FIG. 5.** Derivation of an extended Joukowski relation for the changes in head and velocity across a travelling surge for the case of a finite shutdown time. Here  $\phi(t/\tau)$  is the velocity profile at  $x = 0$  during the shutdown period  $0 \leq t \leq \tau$ .  $D_0$  is the subsequent surge zone in  $x, t$  space.

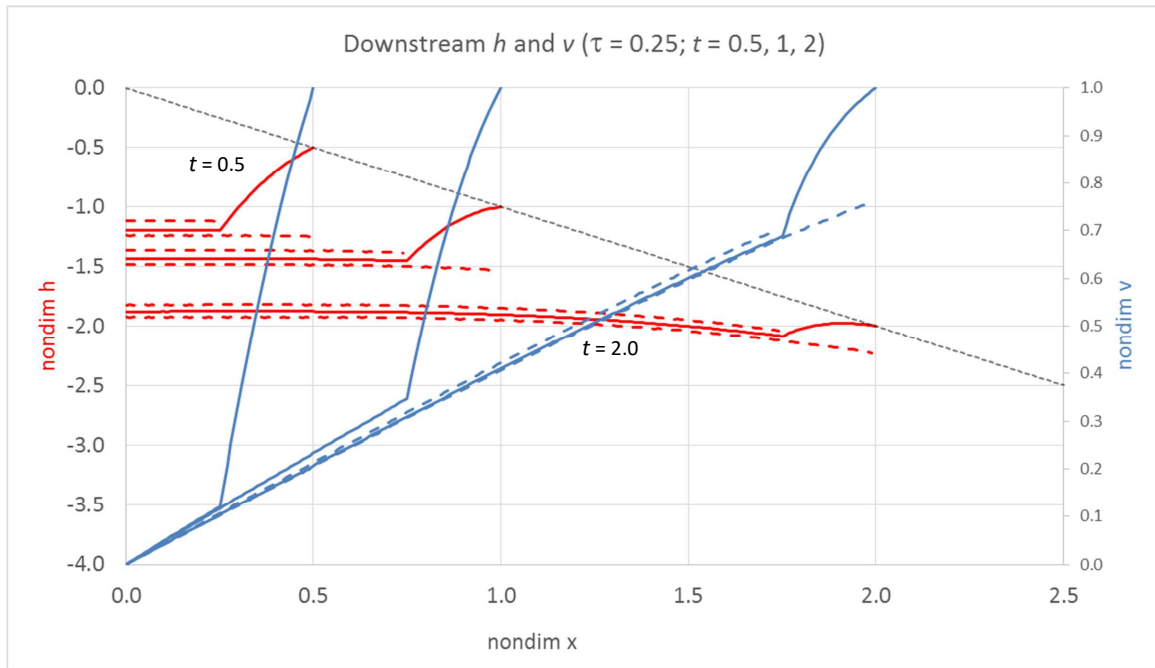


**FIG. 6.** Plots of the downstream  $h$  (red) and  $v$  (blue) for a finite shutdown time of  $\tau = 0.25$ . (A linear shutdown velocity profile  $\phi$  has been assumed.) The red and blue dashed lines bracketing the solid lines correspond to instantaneous shutdowns occurring at  $t = 0$  (below) and  $t = \tau$  (above). To prevent clutter in the figure, the discontinuous jumps in  $h$  and  $v$  for the instantaneous shutdowns have not been shown; also, the bracketing curves for velocity are only shown for  $t = 2$ . The dashed black line is the hydraulic grade line,  $h = -x$ .